A Study of Heating and Degradation of Acrylonitrile-Butadiene-Styrene/Polycarbonate

Polymer Due to Ultraviolet Lasers Illumination during Localized Pre-Deposition Heating

for Fused Filament Fabrication 3D Printing

by

Scott Daniel Kusel

A Thesis Presented in Partial Fulfillment
of the Requirements for the Degree
Master of Science

Approved April 2017 by the
Graduate Supervisory Committee:

Keng Hsu, Chair
Angela Sodemann
Arunachala Mada Kannan

ARIZONA STATE UNIVERSITY

May 2017

Abstract

With the growing popularity of 3d printing in recreational, research, and commercial enterprises new techniques and processes are being developed to improve the quality of parts created. Even so, the anisotropic properties is still a major hindrance of parts manufactured in this method. The goal is to produce parts that mimic the strength characteristics of a comparable part of the same design and materials created using injection molding. In achieving this goal the production cost can be reduced by eliminating the initial investment needed for the creation of expensive tooling. This initial investment reduction will allow for a wider variant of products in smaller batch runs to be made available. This thesis implements the use of ultraviolet (UV) illumination for an in-process laser local pre-deposition heating (LLPH). By comparing samples with and without the LLPH process it is determined that applied energy that is absorbed by the polymer is converted to an increase in the interlayer temperature, and resulting in an observed increase in tensile strength over the baseline test samples. The increase in interlayer bonding thus can be considered the dominating factor over polymer degradation.

Acknowledgements

I would like to sincerely thank my advisor, Dr. Keng Hao Hsu for granting me the opportunity to work with him in The Advance Multi-scale Manufacturing Lab. His experience and expertise has been instrumental in guiding me through my work. It is always astonishing the amount of knowledge he has on tap.

I would like to thank Dr. Angela Sodemann, and Dr. Arunachala Mada Kannan for accepting seats on my defense committee I appreciate the time they took out of their busy schedules to help me with my research.

I would like to thank Anagh Deshpande, Abinesh Ravi, Raymond Churchwell, and Mazin Mohammad for taking time away from their own important research in order to help me. I would also like to thank the rest of my lab mates for making an enjoyable working environment.

I would like to thank Scott Almen, Rhett Sweeney, Osama Jameel, and Eduardo Fernandez for their help in creating experimental apparatuses, and allowing me to spend many late nights testing samples.

Finally I would like to thank my family and friends for their support and most importantly their patience as I complete my education.

TABLE OF CONTENTS

LIST OF TABLES

LIST OF FIGURES

1. Introduction

Rapid Prototyping (RP) was originally developed to produce idealized models for physical representations of final parts to be produced in more traditional manufacturing methods. Making model representation of the final part reduces time and costs so that more iterations and refinements can be made resulting in a better design for the final product. As this process was improved, more techniques were implemented, and the field was formally termed Additive Manufacturing (AM). Materials and deposition techniques vary, but AM part creation generally follows the following procedure;

1) Concept generation- Typically from hand sketches.

2) CAD modeling- Using a solid modeling software like SOLIDWORKS, NX, or Inventor, a digital 3D representation of the desired part is created.

3) Solid model slicing- the part file is imported to a "slicing" program such as Simplify3D, Slic3r, or Cura. These programs generated 2D cross-sections at specified intervals normal to the direction of the build platform. From these 2D sections a G-code is compiled including the desired print settings and machine parameters for the "printer" that the part will be created on.

4) Part Creation- The G-code is sent to the print machine where the material is deposited in the 2D cross-sections. Once the layer is complete the distance from the nozzle in which the material is deposited and the completed layer is increased by the amount dictated by the slicing program in the previous step and the next layer is deposited atop. Each 2D layer is built upon the previous layer resulting in a 3D form.

Within the AM field, extrusion-based systems will be the focus of the research work presented in this paper, primarily Fused Filament Fabrication (FFF). Other terms used by this generic process include Melted Extruded Modeling (MEM), Plastic Jet Printing (PJP), and the more commonly referred-to term created by Stratasys, Fused Deposition Modeling (FDM).

1.1. Fused Filament Fabrication

Since 2009 FFF has become more popular, when Stratasys' patent on the FDM process expired. There was upsurge in popularity, and online groups such as the RepRap community began to form as machines became more affordable. The typical FFF process begins when a spool of thermoplastic filament is drawn into a heating block, where the temperature of the filament is increased to its glass transition state. In this viscus state the plastic is extruded through a nozzle to the desired location in the build area. The mass flow of this thermoplastic is controlled by pressure created by the solid filament as it is fed into the heat block via the extruder. Most extruders are comprised of two rollers positioned on either side of the filament. One or both rollers are driven by an electric motor. Tension between these rollers is usually adjustable to regulate the amount of friction applied to the filament. If the fiction is too light the rollers will slip, too much and the filament may deform causing blockage, or sever the filament entirely. To control heat within the system the filament it also fed through a cooling block positioned ahead of the heating block to maintain the solidity of the filament, thus preventing feeding issues contributed by the

softening of the filament. The motion of the nozzle relative to the build plate is controlled by motor inputs calculated by the printer's microprocessor from the G-code tool paths created by the slicing program.

The nature of the build process does present issues with structural integrity of the printed part. The interlayer strength is inherently weaker when compared to the filament strength which is why parts produced this way display anisotropic properties. To counter this it has become common practice to alternate the extrusion rows orthogonally to each other in alternating layers. Doing this yields a part with properties more consistent to a truly isotropic part in the X-axis and Y-axis directions with strengths closer to the material properties.

The parts also display a "ribbed" outer surface as the cylindrical extrusion is laid upon the previous deposition. The effects of this layering process can be reduced by adjusting print parameters such as extruder temperature, build environment temperature, layer height and the rate of material extrusion. While the ribs may be unwanted due to aesthetic reasons they also pose a structural issue, as the two rounded surfaces join each other at a point. The intersection of cylindrical filament extrusion paths can also become enclosed within the volume of the part creating air pockets. Again the formations of the voids can be reduced by adjusting the aforementioned print settings, but both of these flaws concentrate stress to the already weaker interlayer bonds.

These effects can be minimized by the adjustment of the print settings and orienting known high stress regions of the part in a manner to take advantage of the isotropic X-Y plane. However, they are still a major challenge, impeding the expansion of functional FFF

printed consumer products. In that matter lies the scope for this thesis to discover new ways to improve printed part quality and help the technology move forward.

2. Literature Review

There is extensive research in regards to FFF material properties and uniformity. These papers investigate the optimization of multiple process parameters including but not limited to, print volume temperatures, layer heights, tool paths, and extruder temperatures in order to improve mechanical characteristics of FFF printed parts [2-19]. While certain characteristics can be improved it is most likely at the expense of another.

Loads placed on FFF parts normal to the build direction exhibit a 10-65% tensile strength to parts with oriented filament rows parallel to the applied load [21]. The interlayer strength of a FFF part is dictated by temperature and diffusion of the polymer chains across interlayers faces [22-23]. The interlayer bond formations is heavily influenced by the polymer interface healing process as discussed by DeGennes and Wool [25-26]. Interface healing occurs when polymers on both sides of a junction perform wetting, diffusion, and randomization. Once healed the junction between the two faces become indistinguishable. If this can be achieved in a FFF printed part the orientation in which it was constructed would no longer have an effect on the strength and can be considered isotropic.

The previous work performed by Hsu and Ravi explored this healing process by incorporating an infrared laser in to the build process to inject heat directly onto the layer interface. The outcome proved that LLPH increased the interlayer temperature resulting in a greater strength and higher ductility [1]. It can be noted that this process will only work with polymers that contained a pigment or other additive that would absorb infrared light

4

energy, such as carbon black, as the infrared energy is not absorbed by the polymer itself. To expand the range of materials to be used the transmission spectrum of different polymer-matrices, such as acrylonitrile butadiene styrene (ABS) and polycarbonate (PC), were analyzed. Typically the absorption percentage of the light energy is quite high until the range of ultraviolet where there is a sharp decrease. By utilizing a laser within the range of higher absorption, the efficiency at which the increased energy applied to the substrate is increased. This greater energy absorption will either result in an increase in temperature, or the scissoring and cross-linking of the molecular chains of the polymer. Because of its proximity to this range in the spectrum a 404nm laser diode was selected to determine which of these factors has a greater role in the strength of the printed part.

3. Goal of Thesis

Given the low visible to near-IR wavelength absorption issues existing most engineering polymers, an approach to increase absorption of optical energy in un-filled polymers, an approach of shifting heating laser wavelength to near-UV is proposed. However, the effectiveness of UV illumination on polymer surfaces hinges on the mode of energy into which photon energy is coupled. When UV photons impinge on polymer surfaces, the photon energy can (1) be coupled into vibration modes of atomic bonds within monomer, or (2) be coupled into the vibration of monomers themselves. It is vital to determining the relative effect of both to determine the effectiveness of using UV in the LLPH approach.

The hypothesis in our study is, therefore, that the interaction of ultraviolet (UV) laser illumination during the LLPH process will result in the interlayer strength increasing at a greater rate than polymer degradation caused by molecular chain scissoring and cross-linking. We will experimentally determine the effect of heating and degradation by implementing a dual lasers array on a desktop 3D printer the energy can be directed to pre-deposition and post-deposition along the X-axis of travel to provide a larger coverage of the movements of the nozzle during operation.

The rest of this paper documents the procedures for the tensile testing, and surface morphology using SEM images. A discussion of observed results will determine is process can be considered feasible, and will be followed by recommendations for future work.

4. Design of Experiment

4.1. Machine Selection

Machine selection was important to give a good foundation to build the experimental apparatuses. The Type A Machines Series 1 Pro was selected for the following reasons; Cartesian based orientation with the X-axis motion and the Y-axis motion in the same plane which reduces the complexity of the laser fixture. The sturdy all metal frame to resist unwanted vibrations. Heated bed and all metal hotend design allow for a greater range of thermoplastic materials to be studied. Linear rails provide smooth and accurate motion. Modification friendly warranty should and of the stock components suffer from reliability issues.

4.2. Test Coupon Design

To compare the effect of the UV radiation emission to the material the test coupon was designed to undergo tensile loading test. In Figure 1 a CAD model created using SOLIDWORKS.
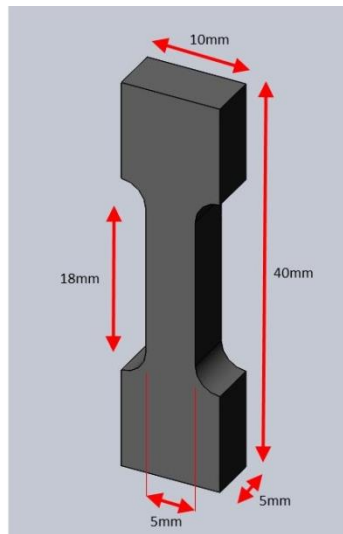

Figure 1: CAD model of test coupon

The configuration is dog-bone in shape with the dimension of 40mm in length, 10mm width, 5mm thickness, 5mm gauge width, and an 18mm gauge length. The slender profile in the center ensures a break near the middle of the part away from the mounting jaws of the tensile tester machine.

4.3. Print Setting Selection

Print settings were chosen in the follow manner. A 20mm wide, 20mm thick, 70mm length block was drawn in SOLIDWORKS and imported in to Simpify3D. The block was set to print as a single wall entity and a spiral outer layer with the extruder temperature initially set to 270^0C the lower temperature limit as specified by the filament manufacturer. Every 10mm of the print the extruder temperature was set to increase by 5^0C until the upper temperature limit of 300^0C as specified by the manufacturer was reached. Upon completion the block was visually inspected for print quality consisting of layer adhesion, discoloration, material clumping, and voids. Next to determine the extrusion multiplier another block of similar dimensions and print setting is printed at the newly established extruder temperature. The extrusion multiplier is initially set at 85% and increased by 5% every 10mm until 115%. Once again the block is visually inspected and the setting that yielded the highest quality is selected. To promote bed adhesion the bed temperature was set to 125^0C, 3M Scotch-Blue painters tape was applied to the glass surface along with a coating of Elmer's All Purpose Glue Stick. Several verification prints were completed with the new settings to confirm part quality. Table 1 outlines the full set of print settings for the test coupons.

Print Parameters	Values
Nozzle Diameter	0.4mm
Extrusion Multiplier	90%
Retraction Distance	3.0mm
Retraction Vertical Lift	1.0mm
Retraction Speed	2400.0mm/min
Layer Height	0.2mm
Top Solid Layer	3
Bottom Solid Layers	3
Shells	0
Skirt	Yes
Raft	Yes
Infill Pattern	Rectilinear
Interior Fill Percentage	100%
Outline Overlap	20%
Infill Extrusion Width	100%
Minimum Infill Length	3.0mm
Infill Angle Offsets	0
Primary Extruder Temp	285c
Heated Bed Temp	120c
Fan Speed	255
Default Printing Speeds	300, 600, 900 mm/min
Outline Underspeed	60%
Solid infill Underspeed	100%
Filament Diameter	1.75mm

4.4. Fixture Design

The laser diode sourced is a 404nm solid-state laser with and output power of 400mW, housed in and adjustable laser diode collimation tube. With this compact packaging multiple laser diodes and housings can be mounted to the print-head and angled to provide an unobstructed line of sight to within 1mm of the extruded material. Figure 2 shows a CAD representation of the laser array assembly mounted to the existing print-head with the four laser diode assemblies installed, but only two were utilized for this group of experiments.
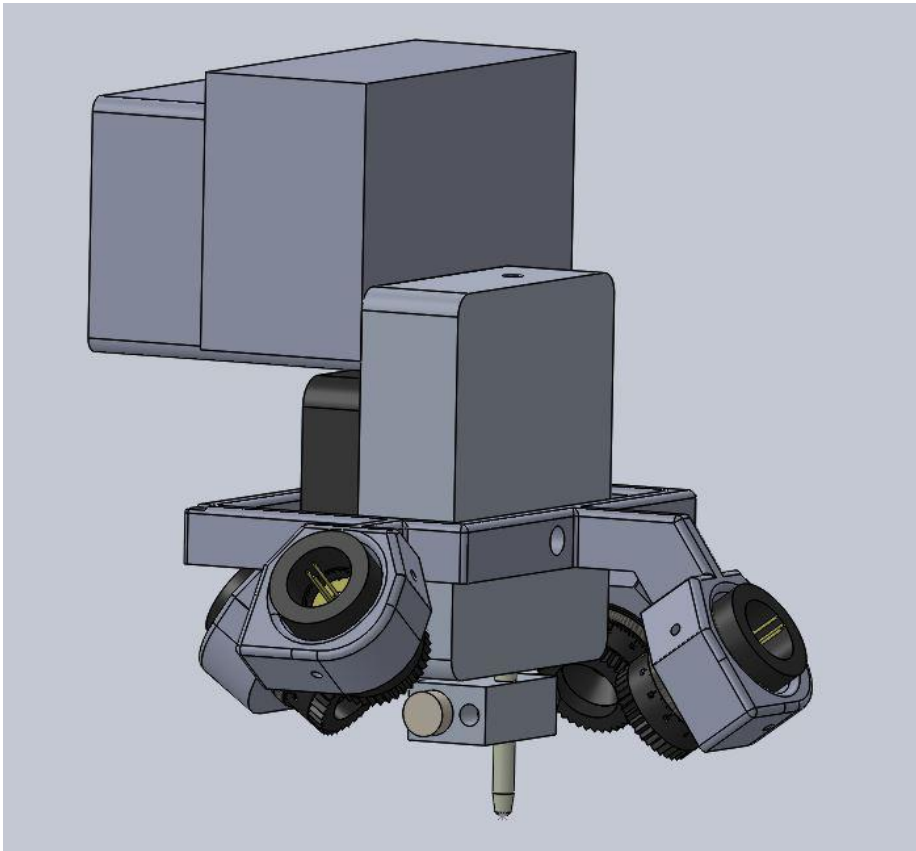

Figure 2: CAD Model of Laser Array Assembly

4.5. Establish Material Properties Baselines

In order to establish a baseline a test coupon specified in Figure 1 is oriented with the broad side flat against the print bed. Doing this will align the extruded filament path in the axial direction of the part. This orientation places less stress on the interlayer-bond as the force carried the continuous material pathway, resulting in a tensile ultimate strength closer to that of an injection molded part of the same material. Table 2 outlines the speed, number of sample, and laser power used for the material baseline.

Table 2: Material Baseline Samples

Print Speed (mm/s)	Number of Sample	Laser Power (mW/laser)
10	5	0
10	5	363

4.6. Varying Energy Density

There are two main factors in the Energy Density (ED) the laser radiates to the material substrate. The first is the print speed, since the lasers are mounted to the print head the ED applied will be inversely proportional to the velocity. The second is the laser power which is directly proportional to the ED. Three groups of samples were created. Each group the print speed was held constant 5mm/s, 10mm/s, and 15mm/s. Within each group the laser power was adjusted to five different settings 0mW/laser, 100mW/laser, 200mW/laser, 300mW/laser, and 363mW/laser. Five samples were printed for each power level. Table 3 outlines the part build parameters created for each group.

11

Group	Print Speed (mm/s)	Number of Samples	Laser Power (mW/laser)
1	5	5	0
1	5	5	100
1	5	5	200
1	5	5	300
1	5	5	363
2	10	5	0
2	10	5	100
2	10	5	200
2	10	5	300
2	10	5	363
3	15	5	0
3	15	5	100
3	15	5	200
3	15	5	300
3	15	5	363

4.7. Interlayer Failure Behavior

By performing tensile stress test on the sample coupons using an Instron 3300 Single Column Universal Testing System, test data will be logged. This data will be further analyzed in-depth will be performed to compare test sample fracture behavior to baselines.

4.8. Fracture Surface Morphology

In order to closer analyze the fractured surfaces coupons Scanning Electron Microscope (SEM) was utilized. The parts first underwent titanium sputtering deposition. This thin layer of conductive titanium prevented the part from becoming charge with the electron beam allowing for a cleaner image. The magnified images will help determine if polymer diffusion has occurred.

5. Results and Discussion

Figure 3 displays results from the tensile stress test of the samples of the baseline FFF process and the LLPH FFF process. Both samples were printed at the 15mm/s, the latter with laser power 363mW per laser. Results show a slight increase of approximately 11% between the two sample averages max tensile stress in favor of the laser treated sample. With the only difference between these two samples being the added laser energy the increase in strength can be contributed to a greater interlayer temperature which promoted diffusion of the polymer chains across the surface interfaces. This is an indication that the absorbed energy from the laser that is converted into heating the polymer has greater effect on the overall part strength than the energy that is converted to scission and cross-linking. Both samples still show brittle fracture behavior evident by the sharp transition from the linear increase in stress to the vertical drop off as the part failed.

The plateau of the strain-strain that occurs between the 5-7Mpa was observed in all test samples performed on this particular Instron tensile machine and is a characteristic of the machine itself and not the print process. It can also be noted that there is spread in the maximum tensile stress between samples within the same group. The FFF process is a dynamic and with variations of diameter and quality of the print media it is possible for different defects to occur. These defects are non-uniform and can vary layer by layer causing weak points in the print, thus causing variation in the of the maximum stress observed.
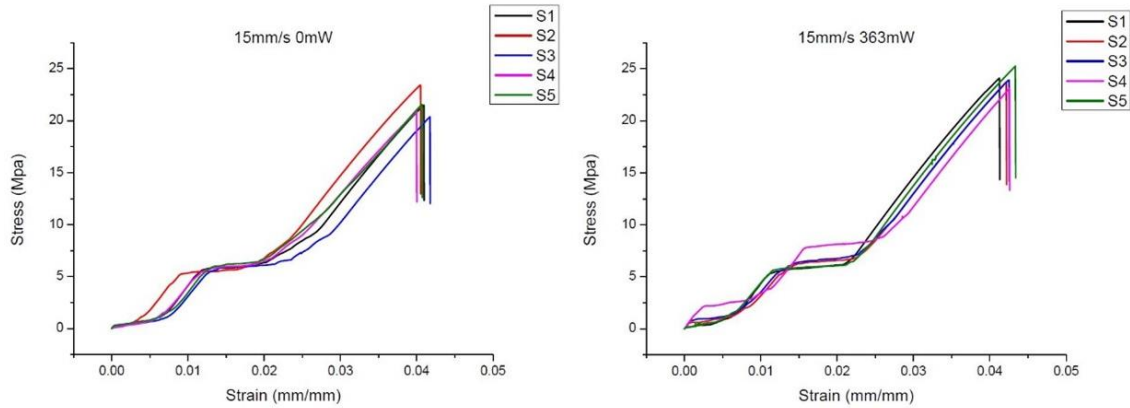
14

Figure 3: Stress Strain Plot for 0mW, and 363mW at 15mm/s

Figure 4 is a consolidation of the 3 print groups, including data for each power setting ranging from 0-363mW per laser. It is apparent from the baseline data from each group that there is a natural increase in the average maximum stress recorded. This can be attributed to the decrease in time it takes to complete one layer of the print before the nozzle deposits the next layer. This decrease in time means less energy is dissipated due to heat transfer allowing the previous layer to maintain a higher interface temperature, increasing the possibility for interlayer diffusion. As the polymers chains diffuse across the interface the material heals and the strength become more of a factor of the material properties than the defects of the surface interactions. It can also be noted that each group has an overall increasing trend as the laser power is increased. This upwards trend indicates that the energy UV laser illuminated on the surface is being converted to heating the substrate promoting diffusion at greater rate than the polymer degradation is occurring. As both of the modes of energy conversions are taking place simultaneously the net sum of the effects results in a positive strengthening the interlayer bonds. As the power of the laser is

15

increased the amount of scission and eventually crosslinking will also increase. The increase in crosslinking will result in the polymer chains being less able to slide past each other reducing ductility. With less plastic deformation generally the effects of defects print defect become more pronounced and part strength is decreased.
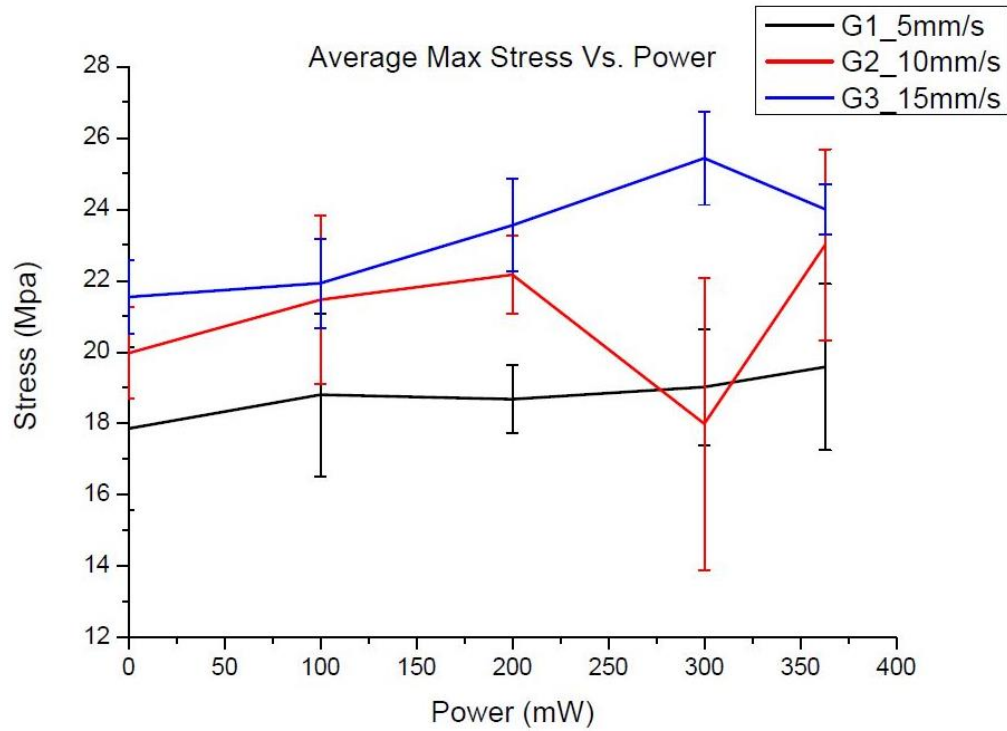

Figure 4: Average Max Stress

When Figures 5 and 6 are compared there is a considerate difference in the appearance of the surface of the fractures. Figure 5 is printed at 5mm/s, and Figure 6 at 10mm/s, both have a laser power setting of 0mW. From this it can be determined that the air pockets in Figure 6 cannot be attributed to the UV laser. The smooth surface in Figure 5 shows that little to no interlayer diffusion as there are no signs of feathering which are present in Figure 6. When the averages of the 10mm/s 0mW sub-group is compared to the 5mm/s 0mW there is a 12% increase in the maximum stress as the speed is increased even with the decrease surface area due to the air pockets.
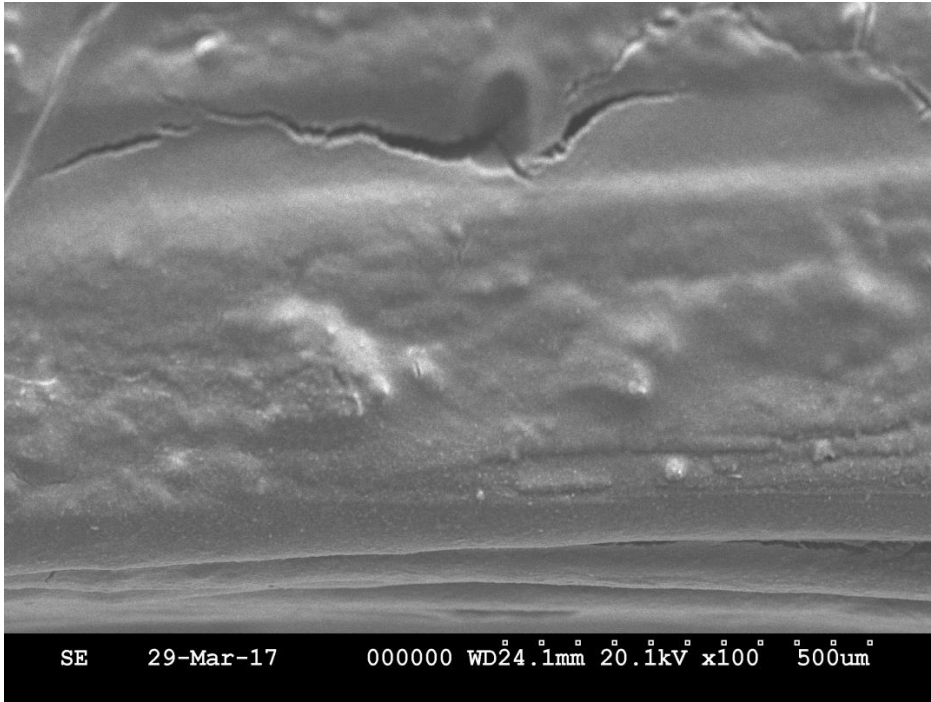
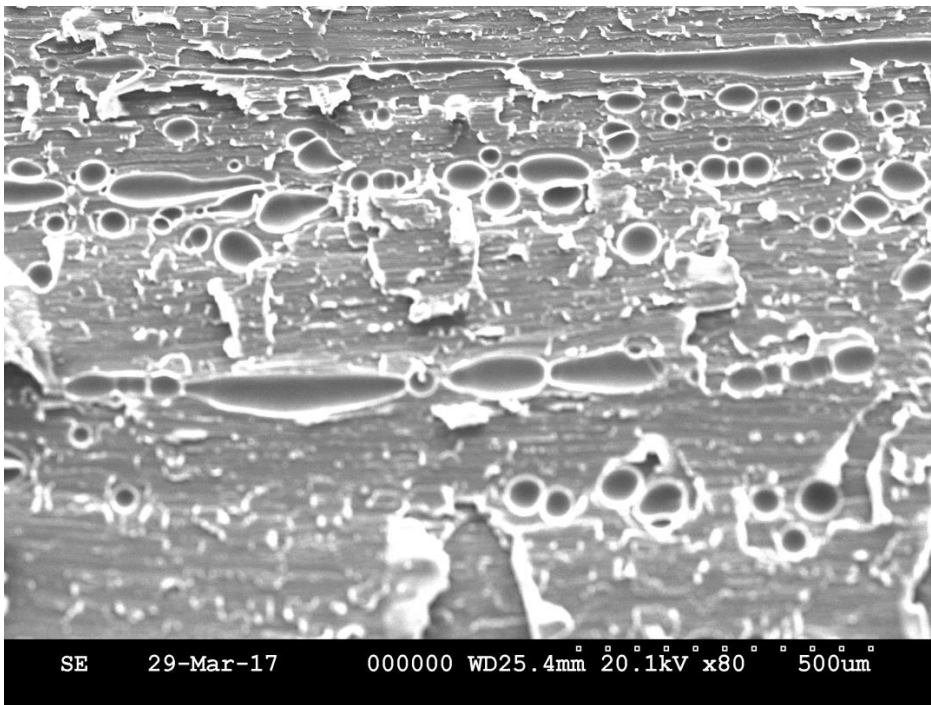*Figure 5: 5mm/s 0mW Surface Morphology*

Figure 6:10mm/s 0mW Surface Morphology

Figures 7 and 8 are printed at 15mm/s and a noticeable increase in the density of the air pockets when compared to Figure 6. Figure 7 is print without laser power while Figure 8 has a setting of 363mW per laser. When compared it appears the interface between the extrusion pathways has been smooth down by the pre-deposition laser. This could indicate that the LLPH process not only aid in the interlayer vertically between the previous layer and a new deposition over the top but also aid in the side-to-side diffusion with parallel rows.
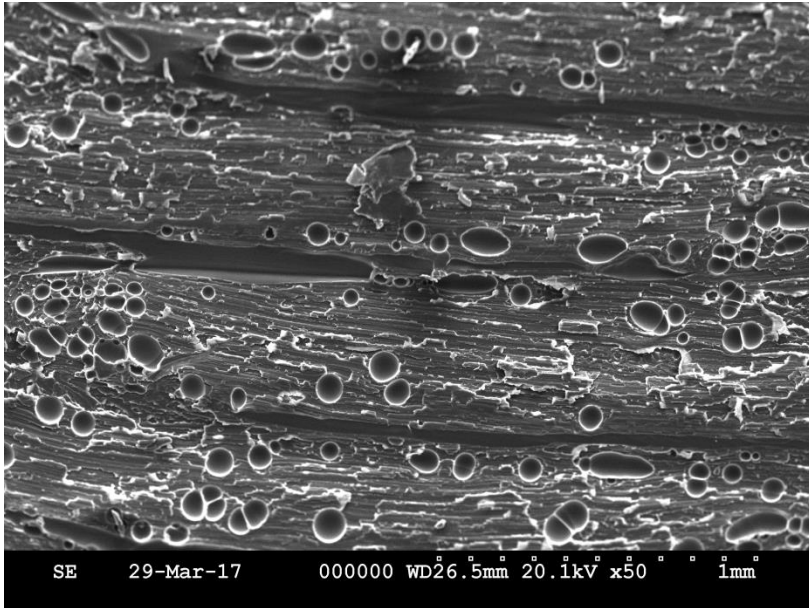
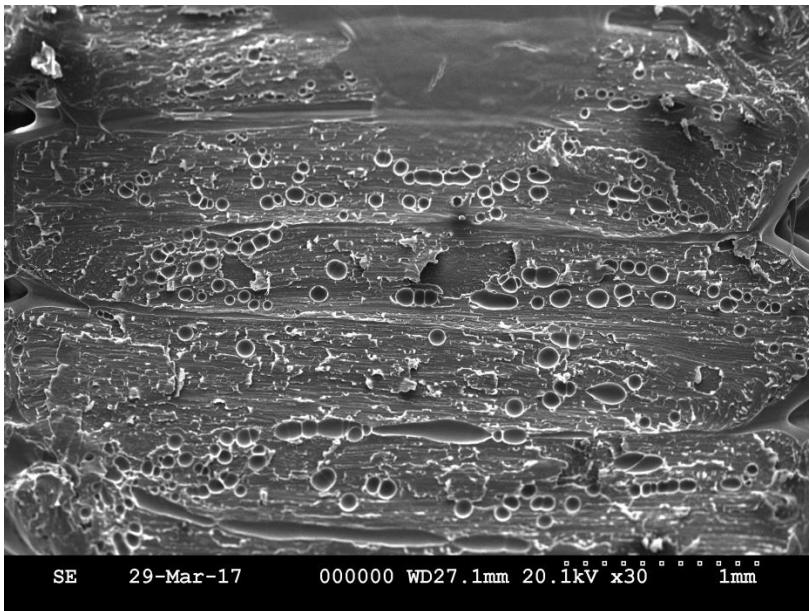*Figure 7: 15mm/s 0mW per laser Surface Morphology*

Figure 8: 15mm/s 363mW per laser Surface Morphology

Conclusion

After comparing the maximum tensile strengths of the baseline FFF 3d printed coupons with those in which the in-process localized ultraviolet laser heating process. A clear trend is observed that the illumination energy applied by the lasers not only did not diminished the strength of the printed parts but actually improved maximum tensile stress in spite of the increase number of air pockets within the printed part due to other unknown parameters. From this we can derive that the UV energy absorbed and converted in to stronger interlayer bonds is more beneficial than the amount of energy that is converted in to polymer material degradation.is harmful to the 3d printed part.

Future Work

The results observed from the SEM were unexpected. Tracking down the source of the air pockets and rerunning the experiments would prove beneficial to the further understanding of the LLPH with UV laser process. Due to the standard deviation seen with in the data replacing the tensile break with the 3-point bend test should possibly yield better results. Also with the incorporation of data from tests like the Road Geometry Analysis and Embedded Interface Temperature Readings it would possible to make a more definitive statement of the effectiveness of the UV laser.

References

1. Ravi A, Deshpande A, Hsu K (2016) An in-process laser localized pre-deposition heating approach to inter-layer bond strengthening in extrusion based polymer additive manufacturing. J Manufacturing processes 24(7):179-185

2. Anitha R, Arunachalam S, Radhakrishnan P (2001) Critical parameters influencing the quality of prototypes in fused deposition modelling. J Mater Process Technol 118(1–3):385–388

3. Nancharaiah T, Raju DR, Raju VR (2010) An experimental investigation on surface quality and dimensional accuracy of FDM components. Int J Emerg Technol 1(2):106–111

4. Thrimurthulu K, Pandey PM, Reddy NV (2004) Optimum part deposition orientation in fused deposition modeling. Int J Mach Tools Manuf 44(6):585–594

5. Horvath D, Noorani R, Mendelson M (2007) Improvement of surface roughness on ABS 400 polymer using design of experiments (DOE). Mater Sci Forum 561:2389–2392

6. Wang CC, Lin TW, Hu SS (2007) Optimizing the rapid prototyping process by integrating the Taguchi method with the gray relational analysis. Rapid Prototyp J 13(5):304–315

7. Sood AK, Ohdar R, Mahapatra S (2009) Improving dimensional accuracy of fused deposition modelling processed part using grey Taguchi method. Mater Des 30(10):4243–4252

8. Zhang JW, Peng AH (2012) Process-parameter optimization for fused deposition modeling based on Taguchi method. Adv Mater Res 538:444–447

9. Sahu RK, Mahapatra S, Sood AK (2013) A study on dimensional accuracy of fused deposition modeling (FDM) processed parts using fuzzy logic. J Manuf Sci Prod 13(3):183–197

10. Lee B, Abdullah J, Khan Z (2005) Optimization of rapid prototyping parameters for production of flexible ABS object. J Mater Process Technol 169(1):54–61

11. Laeng J, Khan ZA, Khu SY (2006) Optimizing flexible behavior of bow prototype using Taguchi approach. J Appl Sci 6:622–630

12. Zhang Y, Chou K (2008) A parametric study of part distortions in fused deposition modelling using three-dimensional finite element analysis. Proc Inst Mech Eng Part B 222(8):959–968

13. Nancharaiah T (2011) Optimization of process parameters in FDM process using design of experiments. Int J Emerg Technol 2(1):100–102

14. Kumar GP, Regalla SP (2012) Optimization of support material and build time in fused deposition modeling (FDM). Appl Mech Mater 110:2245–2251

15. Ahn SH, Montero M, Odell D et al (2002) Anisotropic material properties of fused deposition modeling ABS. Rapid Prototyp J 8(4):248–257

16. Ang KC, Leong KF, Chua CK et al (2006) Investigation of the mechanical properties and porosity relationships in fused deposition modelling-fabricated porous structures. Rapid Prototyp J 12(2):100–105

17. Sood AK, Ohdar RK, Mahapatra SS (2010) Parametric appraisal of mechanical property of fused deposition modelling processed parts. Mater Des 31(1):287–295

18. Percoco G, Lavecchia F, Galantucci LM (2012) Compressive properties of FDM rapid prototypes treated with a low cost chemical finishing. Res J Appl Sci Eng Technol 4(19):3838–3842

19. Rayegani F, Onwubolu GC (2014) Fused deposition modelling (FDM) process parameter prediction and optimization using group method for data handling (GMDH) and differential evolution (DE). Int J Adv Manuf Technol 73(1–4):509–519

20. Masood SH, Mau K, Song WQ (2010) Tensile properties of processed FDM polycarbonate material. Mater Sci Forum 654:2556–2559

21. Sung-Hoon Ahn, Michael Montero, Dan Odell, Shad Roundy, and Paul K. Wright, Anisotropic material properties of fused deposition modeling ABS, Rapid Prototyping, Vol. 8, No. 4, 2002, PP248.

22. Rodriguez, J.F., Thomas, J.P. and Renaud, J.E., "Tailoring the mechanical properties of fused-deposition manufactured components", *Proc. Rapid Prototyping and Manufacturing '99*, Vol. 3, Society of Manufacturing Engineers, Dearborn, MI, pp.629-43. (1999)

23. Yan, Y., Zhang, R., Guodong, H., and Yuan, X., "Research on the bonding of material paths in melted extrusion modeling", *Materials and Design*, Vol. 21, pp. 93-99. (2000)

24. Seth Partain, Fused Deposition Modeling with Localized Pre-Deposition Heating Using Forced Air, Master's Thesis, Montana State University, 2007

25. P. G. De Gennes, " Reptation of a polymer chain in the presense of fixed obstacles," the Journal of Chemical Physics, 572, 1971.

26. Wool, R.P., Yuan, B.L. and MacGarel, J., "welding of polymer interfaces," Journal of Polymer Engineering and Acience, V.29, pp. 1340 (1989)